



Published in final edited form as:

Adv Exp Med Biol. 2006 ; 578: 119–124.

IMAGING OXYGEN PRESSURE IN THE RODENT RETINA BY PHOSPHORESCENCE LIFETIME

David F. Wilson^a, Sergei A. Vinogradov^a, Pavel Grosul^a, Newman Sund^b, M. Noel Vacarezza^a, and Jean Bennett^b

^aDepartment of Biochemistry and Biophysics, Medical School, University of Pennsylvania, Philadelphia, PA 19104

^bDepartment of Ophthalmology, Medical School, University of Pennsylvania, Philadelphia, PA 19104

1. INTRODUCTION

Many diseases of the eye, especially those causing inner retinal neovascularization (diabetic retinopathy, retinopathy of prematurity, sickle cell disease, etc.) have regional hypoxia as either a primary causative or early contributory factor. This is particularly true for diabetic retinopathy, the leading cause of blindness for individuals between 20 and 74 years of age. In diabetes, multiple structures of the eye are pathologically affected by vascular changes with resultant plasma leakage and tissue disruption (1). Currently available data suggest that the pathological growth of new vessels results from developing regions of hypoxia in the retina. These new blood vessels in the inner retina are defective and exude from the vessels and/or bleeding due to vessel rupture are the major cause of the decreased vision/blindness associated with diabetes. Using microelectrodes, Linsenmeier and coworkers (2,3), reported that in diabetic cats the oxygen pressures in the inner half of the retina are about one half those of normal cats, and Berkowitz et al. (4), reported decreased oxygen response in the retina of galactosemic rats. Oxygen electrodes can very effectively identify global oxygen deficiency but are invasive. Also, since they make point measurements, they are not very effective for measuring focal hypoxia induced through microvessel failure. Retinal pathology in diabetes, for example, is thought to begin with pathological changes in the intraretinal microvessels (nonproliferative diabetic retinopathy) to growth of new vessels in the extraretinal space⁵. Similar pathogenic mechanisms are thought to occur in other diseases characterized by inner retinal neovascularization. Hypoxia resulting from vascular insufficiency could be responsible for production of high levels of vascular endothelial growth factor (VEGF). Vitreous samples in humans with retinopathy have contained high levels of VEGF (5). High levels of VEGF have also been measured in animal models of ocular neovascular disease (see 6,7,8).

In the present paper, we report continuing progress (see 9) in developing a phosphorescence lifetime imaging system capable of obtaining high resolution images of the oxygen distribution in the retina of the rodent eye. These oxygen measurements would make possible critical evaluation of the role of microcirculatory failure in vision loss using a variety of rodent models for human disease.

2. METHODS

2.1. Phosphorescence Lifetime Imaging System

The phosphorescence lifetime imaging system previously used to image oxygen in the retina of the cat eye (10,11) was modified to allow imaging of phosphorescence lifetimes in the much smaller mouse eye following the lead of Shonat and Kight (12,13). A frequency domain approach (14, 15) was used in which the excitation light source was modulated in a square wave while the gate of the intensified CCD camera was similarly modulated but delayed with respect to the excitation. On axis illumination was achieved by placing a dichroic mirror in the optical path and using it to reflect the excitation light into the optical path. Long working distance (18 mm) microscope optics were used between the dichroic mirror and the eye. A Xybion ISG 750 camera (now ITT Night Vision, Roanoke, VA) with enhanced red sensitivity was used for imaging the phosphorescence. The intensifier of this camera can be turned on or off “gated” in approximately 0.10 μ sec. The excitation light source is a high power LED with a response time of less than 1 microsecond. Both the camera intensifier and the LED are modulated in square waves with a 50% duty cycle at frequencies from less than 100 Hz to greater than 40,000 Hz. In order to determine the phosphorescence lifetime, phosphorescence intensity images are collected at 7 to 10 different delays over the range from 0 to 360 degrees relative to the excitation light. These are then analyzed by fitting the intensity at each pixel of the image set to a sinusoid of the frequency used for taking the images. The phase of the phosphorescence relative to the excitation is determined and from the phase shift and frequency, the phosphorescence lifetime is calculated. The quenching by oxygen follows the Stern-Volmer relationship:

$$T^0/T = 1 + k_Q * T^0 * pO_2 \quad (1)$$

where T^0 and T are the phosphorescence lifetimes at oxygen pressures (pO_2) of zero and the experimental value, respectively, and k_Q is a second order rate constant related to the frequency of collision of excited state phosphor molecules with molecular oxygen and the probability that energy transfer will occur in each collision. Equation 1 makes it possible to calculate the oxygen pressure at each pixel of the image array once the phosphorescence lifetime is known.

The imaging software calculates the best fit of the data from each pixel of the image array and generates pixel by pixel maps of: 1. phase delay (phase shift) of the emission relative to the excitation light. 2. goodness of fit to a sinusoid as given by the regression coefficient ($r = 1.0$ is a perfect fit); 3. phosphorescence lifetime; and 4. oxygen pressure as calculated from eq. 1. In living tissue, there can be significant tissue auto-fluorescence and/or leakage of excitation light through the optical filters. These signals occur with an effective phase shift of zero relative to the excitation. If no correction is made, they add to the phosphorescence and result in a progressive decrease in phase shift with increasing fraction of the signal. In order to correct for the “in phase” signal, two additional images are taken at 0 and 180 degrees relative to excitation, but at a frequency of 36 kHz. At such a high frequency the phosphorescence signal is highly demodulated and the remaining signal is phase shifted, relative to excitation, by more than 80 degrees. Thus the difference in image intensity between 0 and 180 degrees approximates the “in phase” signal due to tissue fluorescence and excitation light leak. The phosphorescence signal at each phase delay is corrected for the “in phase” signal and the phosphorescence lifetimes calculated. This correction has been tested with samples containing mixtures of fluorophor and phosphor and shown to effectively remove the effect of the fluorescence as long as it accounted for less than about 50% of the total intensity.

2.2. Experimental Protocol

The pigmented mice were anesthetized by i.p. injection of 0.2 ml of a solution with ketamine (25 mg/ml) and xylazine (25 mg/ml) dissolved in phosphate buffered saline. A drop of 1% tropicamide (Mydracyl®, Alcon, Ft. Worth, TX) was placed on the eyes to dilate the pupils and the Oxyphor G2 (1.6 mg/ml in unbuffered saline, pH 7.5) given by i.v. injection of 0.15 ml into the tail vein. Approximately 4 min after the Mydracyl®, a drop of hydroxypropyl methylcellulose (Goniosol®, CIBA Vision Ophthalmics, Atlanta, GA) was placed on the eye and then a small piece of clear plastic sheet was gently placed on the Goniosol®. The retina was then imaged through the cover slip. Phosphorescence imaging began as early as 3 min after injection of the phosphor and on occasion continued for periods as long as 1.5 hrs.

Oxyphor G2, recently synthesized by Vinogradov and coworkers (16,17) was excited using 450 nm light and the phosphorescence (peak 790 nm) was collected through a 2mm 695 nm long pass Schott glass filter.

3. RESULTS AND DISCUSSION

3.1. Imaging Phosphorescence and Oxygen in the Mouse Retina

Sets of images, suitable for calculation of lifetime and oxygen maps, were taken of phosphorescence from Oxyphor G2 in the blood plasma of the retina. The phosphorescence intensity images show good resolution of the vasculature of the retina. Figure 1 shows phosphorescence images at 30 degrees delay relative to excitation and from the image sets taken 5 and 35 min. after induction of anesthesia and dilation of the pupil. The phosphorescence intensity images are presented as negatives, with increasing intensity appearing as increasing darkness in the image. The images taken just 5 min. after anesthesia show significantly higher intensity from the veins and capillaries relative to the arterioles than do the images taken at 35 min. after anesthesia. This is consistent with the oxygen pressure maps, which show the oxygen pressures in the veins were much lower (15 mm Hg) at 5 min than at 35 min (50 mm Hg).

3.2. Effect of Anesthesia on the Measured Oxygen Maps

In the experiment shown in Fig. 1 and 2, a total of 19 oxygen maps, each consisting of a set of 9 phosphorescence intensity images, were taken over a period of 35 min. The venous oxygen pressures were decreased immediately following anesthesia but recovered in approximately 15 minutes to a stable level. The anesthesia response was quite variable among mice, ranging from no measurable effect (both arteriolar and venous oxygen pressures were stable from the beginning) to intermittent breathing throughout the period of anesthesia. In the latter case, the arteriolar and venous oxygen pressures were both unstable, decreasing during apnea and then quickly rising again when breathing restarted. Oxygen pressures measured in normal muscle tissue on the back leg showed similar effect of anesthesia on the oxygen levels (data not shown). Once the venous oxygen pressures increased to near normal, however, continuing measurements showed no further change. In addition, the oxygen map for the 35 min measurement (Fig. 1D) shows no evidence of local alterations in oxygen pressure, indicating that the measurements *per se* did not result in vascular injury.

3.3. Do the Oxygen Measurements Cause Vascular/Tissue Injury?

Figure 1 and Figure 2 demonstrate that many consecutive measurements of oxygen maps can be made without significant alteration in the measured oxygen pressures or evidence of vascular injury. We have made measurements of the same region of the same eye of individual mice, repeated 3 times at 1 week intervals, 20 measurements (complete oxygen maps) per occasion. No evidence was found for vascular injury even in the 60th measurement. Further experiments are underway to determine at what point there is evidence for retinal injury.

Acknowledgments

Supported in part by NS-31465, HD041484, and R43-DK064543.

REFERENCES

1. L'Esperance, FA.; James, WA. The eye and diabetes Mellitus. In: Ellenberg, M.; Rifkin, H., editors. *Diabetes Mellitus: Theory and Practice*. Vol. ed. 3. New Hyde Park, N. Y.: Med. Examination; 1983. p. 727-757.
2. Linsenmeier RA. Effects of light and darkness on oxygen distribution and consumption in the cat retina. *J. Gen. Physiol* 1986;88:521-542. [PubMed: 3783124]
3. Linsenmeier RA, Braun RD, McRipley MA, Padnick LB, Ahmed J, Hatchell DL, McLeod DS, Luty GA. Retinal hypoxia in long-term diabetic cats. *Invest. Ophthalmol. & Visual Sci* 1998;39:1647-1657. [PubMed: 9699554]
4. Berkowitz BA, Kowluru RA, Frank RN, Kern TS, Hohman TC, Prakash M. Subnormal retinal oxygenation response precedes diabetic-like retinopathy. *Invest. Ophthalmol. & Visual Sci* 1999;40:2100-2105. [PubMed: 10440266]
5. Maguire AM. Management of diabetic retinopathy. *J. Am. Osteopathic Assoc* 1997;97:S6-S11.
6. Adamis AP, Miller JW, Bernal MT, D'Amico DJ, Folkman J, Yeo T-K, Yeo K-T. Increased vascular endothelial growth factor levels in the vitreous of eyes with proliferative diabetic retinopathy. *Am. J. Ophthalmol* 1994;118:445-450. [PubMed: 7943121]
7. Pierce EA, Avery RL, Foley ED, Aiello LP, Smith LEH. Vascular endothelial growth factor/vascular permeability factor expression in a mouse model of retinal neovascularization. *Proc Natl Acad Sci USA* 1995;92:905-909. [PubMed: 7846076]
8. Dorey CK, Aouidid S, Reynaud X, Dvorak HF, Brown LF. Correlation of vascular permeability factor/vascular endothelial growth factor with extraretinal neovascularization in the rat.[comment][erratum appears in *Arch Ophthalmol* 1997 Feb; 115(2):192]. *Arch. Ophthalmol* 1996;114:1210-1217. [PubMed: 8859080]
9. Wilson DF, Vinogradov SA, Grosul P, Kuroki A, Bennett J. Imaging oxygen in the retina of the mouse eye. *Adv. Exptl. Med. Biol.* 2004In press.
10. Shonat RD, Wilson DF, Riva CE, Cranstoun SD. Effect of acute increases in intraocular pressure on intravascular optic nerve head oxygen tension in cats. *Investigative Ophthalmology & Visual Science* 1992;33:3174-3180. [PubMed: 1399424]
11. Shonat RD, Wilson DF, Riva CE, Pawlowski M. Oxygen distribution in the retinal and choroidal vessels of the cat as measured by a new phosphorescence imaging method. *Applied Optics* 1992;33:3711-3718.
12. Shonat RD, Kight AC. Frequency domain imaging of oxygen tension in the mouse retina. *Adv. Exptl. Med. Biol* 2003a;510:243-247. [PubMed: 12580435]
13. Shonat RD, Kight AC. Oxygen tension imaging in the mouse retina. *Ann. Biomed. Eng* 2003b; 31:1084-1096. [PubMed: 14582611]
14. Vinogradov SA, Fernandez-Seara MA, Dugan BW, Wilson DF. Frequency domain instrument for measuring phosphorescence lifetime distributions in heterogeneous samples. *Rev. Sci. Inst* 2001;72 (8):3396-3406.
16. Vinogradov SA, Wilson DF. Metallotetrabenzoporphyrins. New phosphorescent probes for oxygen measurements. *J. Chem. Soc., Perkin Trans* 1994;II:103-111.
17. Dunphy I, Vinogradov SA, Wilson DF. Oxyphor R2 and G2: Phosphors for measuring oxygen by oxygen dependent quenching of phosphorescence. *Analy. Biochem* 2002;310:191-198.

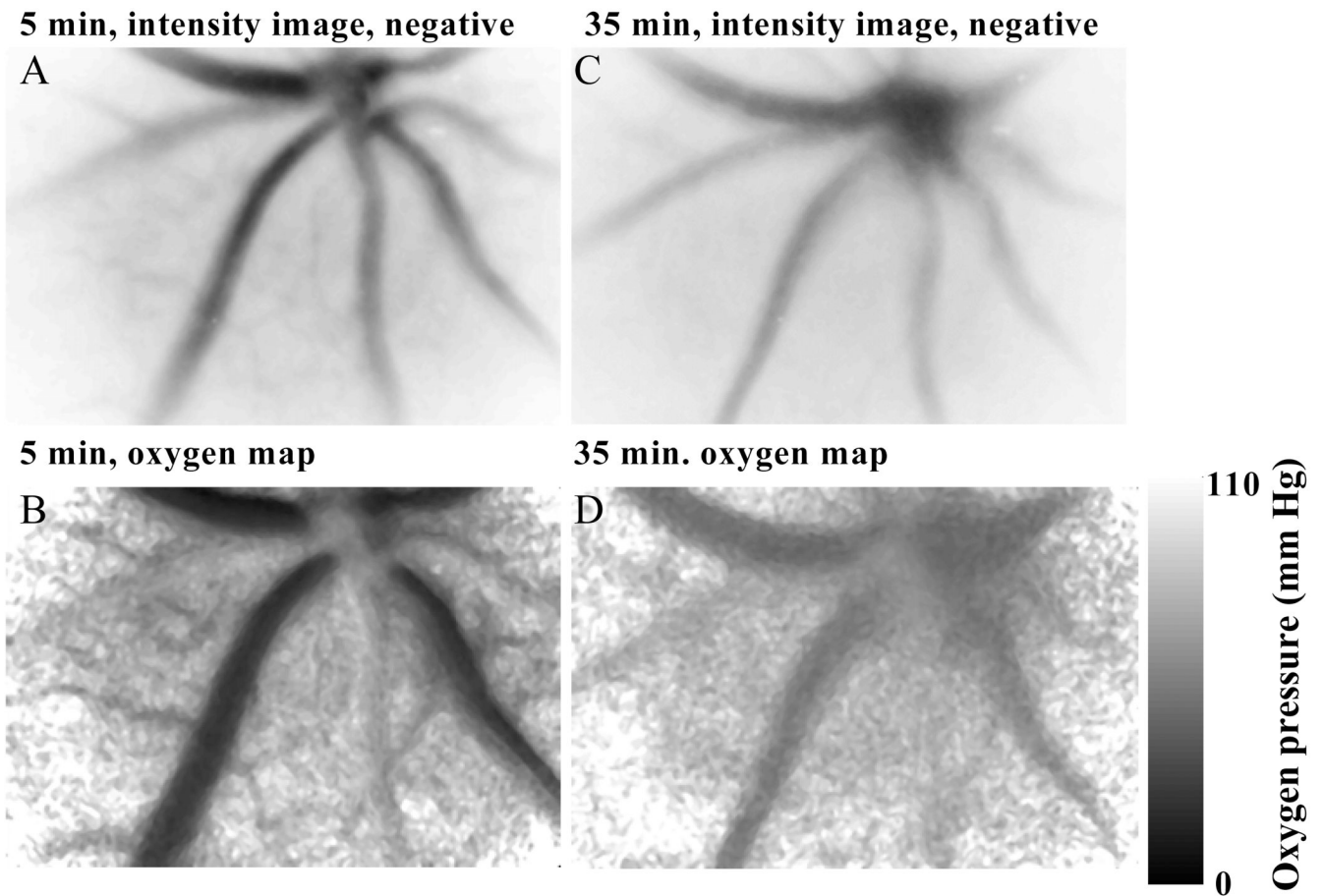


Figure 1.

Dependence of the retinal oxygen pressures on the time after induction of anesthesia. The mouse was given an intraperitoneal injection of anesthetic, the pupil dilated, and retinal imaging of the phosphorescence lifetimes begun about 3 minutes later. The area of the retina that was imaged was approximately 0.92 mm high by 1.2 mm wide. The presented images and oxygen maps are from the data sets taken 5 and 35 min after induction of anesthesia.

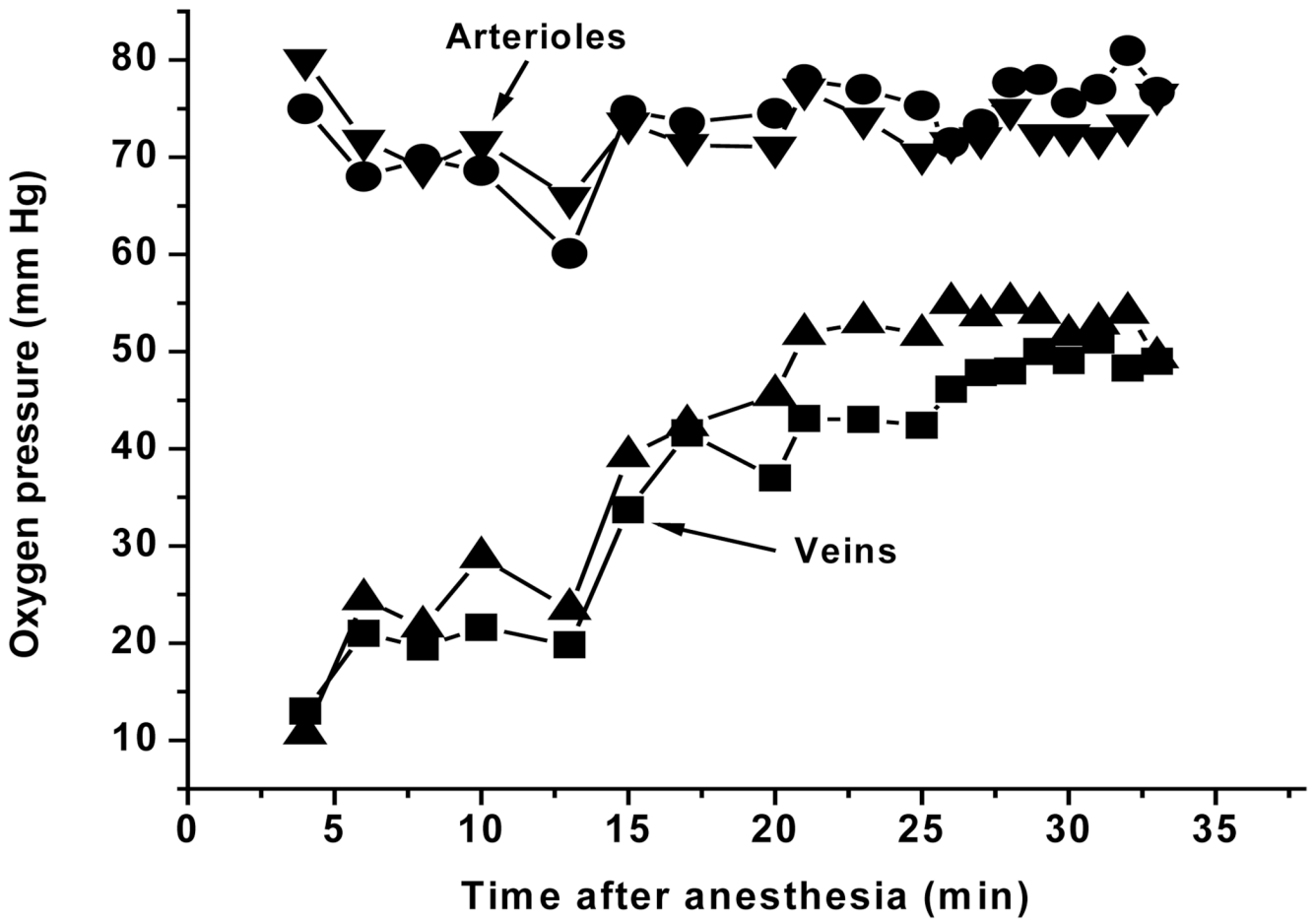


Figure 2.

Time course of the oxygen pressures in the retinal veins and arterioles of the mouse retina following anesthesia. Oxygen pressure maps of the retina were repetitively measured, a total of 19 measurements over the period of 3 to 35 minutes following anesthesia. Regions of interest were selected within two different arterioles and two different veins and the average oxygen pressures for each region determined at every time point. The resulting values are plotted in the figure as a function of the time after anesthesia.